Characterization of GTO's Under Different Modes of Zero Current Switching

Axel Mertens, *Member, IEEE,* Hans-Christoph Skudelny, *Senior Member, IEEE,*
Paulo P. A. Caldeira, *Member, IEEE,* and T. Lipo, *Fellow, IEEE*

***Abstract*—In recent years, several papers described the use of GTO's in zero current switching (ZCS) applications, with the goal of increasing the frequency range for medium- and high-power converters.**

Zero current switching with GTO's can be applied in series and parallel resonant converters, as well as in PWM inverters with commutation aid networks. The voltage and current waveforms at the devices differ in each of these applications, and different modes of ZCS can be identified. In this paper, a comparative view of the behavior and characteristics of the GTO in the different modes of ZCS is presented.

The variety of ZCS waveforms is described and transferred into a unifying schematic. The behavior of GTO's in the different modes of operation is characterized, and requirements to the circuit environment are pointed out. The relations between the most important circuit parameters and some of the device waveform parameters are investigated experimentally.

I. Introduction

At the high end of the power range of today's power electronic equipment, the thyristor and the GTO are still the only devices applicable. The switching frequencies used for generation and control of dc or sinusoidal output voltages and currents are restricted to a few hundred Hertz because of the large turnoff time in thyristor circuits, and the very high switching losses of GTO's. The same characteristics limit the frequency of high-power resonant inverters, which are mainly used in induction heating applications.

A successful approach to reduce thyristor turnoff time was made with the gate-assisted turnoff mode (GATO). With a negative gate voltage applied during the hold-off time, the device can be held in the off state when positive voltage is reapplied, even if a forward recovery current occurs due to the presence of stored charge in the central regions of the device. This current is deviated into the gate, instead of flowing via the gate cathode junction and turning on the device. The effectiveness of this method depends on the gate structure. The turnoff time could be reduced down to about eight microseconds.

It is obvious that the GTO with its much finer gate structure is ideally suited for the gate-assisted turnoff mode, and promises even lower turnoff times and higher frequencies. Several papers were published in recent years describing the use of GTO's in zero current switching applications [1], [2], [5]–[7], [9]–[12]. Some device manufacturers even announced an optimized GTO-like device for such applications, the zero turnoff time thyristor (ZTO) [3], [4].

Zero current switching with GTO's can be applied in all circuits where thyristors have been used. The voltage and current waveforms at the devices differ in many of the applications, and so does the device behavior. Several different modes of zero current switching (ZCS) can be identified.

The characteristics of GTO's under ZCS are much different from the characteristics under normal GTO operation. They also differ from a normal thyristor behavior, because of the different device design (doping, gate structure) and the negative gate current applied for turnoff.

This paper gives a comparative view of the different modes of ZCS with GTO's. The variety of ZCS waveforms is described and transferred into a unifying schematic. The behavior of GTO's in the different modes of operation is characterized and evaluated, and requirements to the circuit environment and operation conditions are pointed out. The most important device characteristics are investigated experimentally.

II. Modes of ZCS Operation

The GTO can be applied in ZCS modes of operation wherever a thyristor can be used. This includes choppers and PWM inverters with commutation aid networks [6], [7], as well as series and parallel resonant converters [1], [2], [9]–[12]. A new ZCS circuit for UPS and drive applications, the resonant dc current link inverter (RDCCLI) has been introduced in [8]. In this circuit, high switching frequencies are required in order to obtain acceptable output waveforms, a drawback which stems from the discrete nature of the current pulses. Fig. 1 shows all of the circuits mentioned above and their basic waveforms.

The different waveforms can be divided into four basic modes of operation (Fig. 2). The current is shaped either sinusoidal (series resonant inverter, resonant dc current link inverter) or trapezoidal (voltage pulse commutation, current pulse commutation, parallel resonant converter). The voltage is either a ramp, starting at negative values (parallel resonant converter, voltage pulse commutation), or it is only slightly negative during the hold-off time and steps to a forward blocking voltage afterwards (all the applications with an antiparallel diode, like series resonant inverter and current

Manuscript received June 25, 1992; revised November 2, 1993.

A. Mertens is with Siemens AG, D-91058 Erlangen, Germany.

H.-C. Skudelny is with RWTH Aachen University of Technology, D-5100 Aachen, Germany.

P. P. A. Caldeira is with the North American Philips Corp., Briarcliff Manor, NY 10510-2099.

T. Lipo is with the University of Wisconsin-Madison, Madison, WI 53706.

IEEE Log Number 9402449.

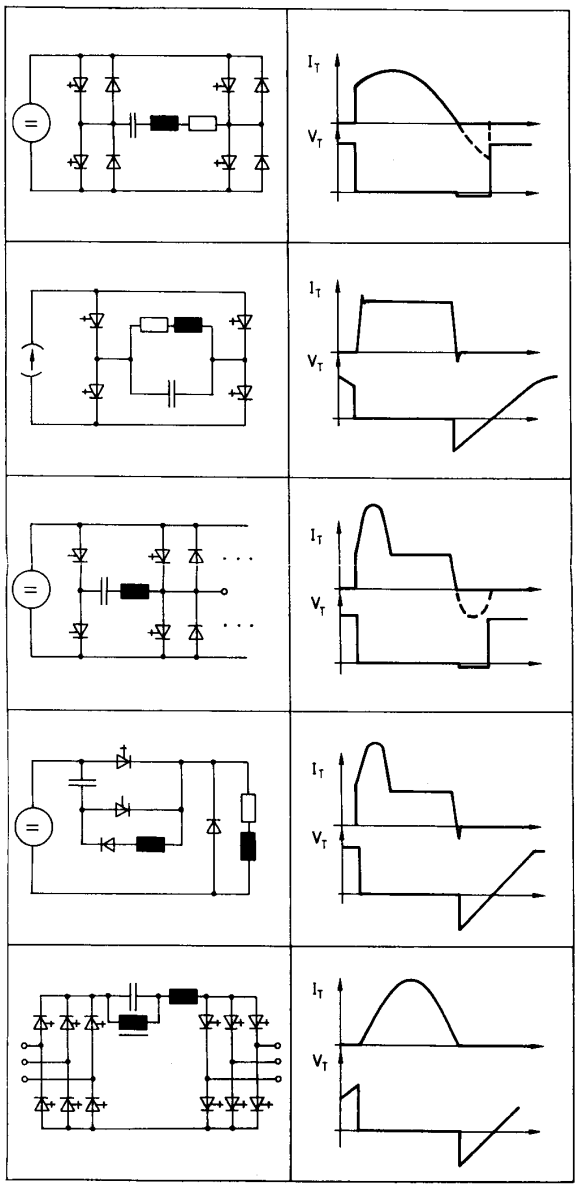

Fig. 1. Different circuits where GTO's can be applied in a ZCS mode of operation: series resonant inverter, parallel resonant converter, PWM inverter and chopper using forced commutation, and resonant dc current link inverter.

pulse commutation). All of the four possible combinations appear in the circuits of Fig. 1.

III. Behavior of GTO's in ZCS

A. General Considerations

On principle, the GTO has a structure similar to a thyristor. Some variations in the design are made in order to achieve gate turnoff capability. This concerns both the gate structure, which has to be highly interdigitated with the cathode, and some precautions to reduce the base transport coefficient of

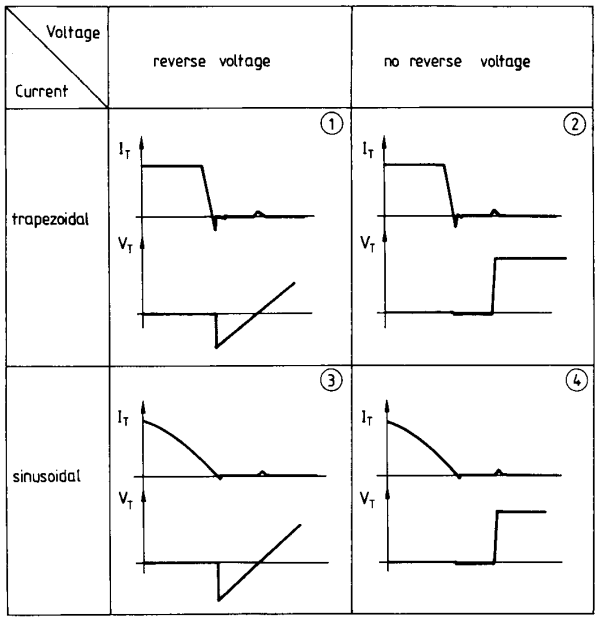

Fig. 2. Basic modes of ZCS.

the anode-side pnp transistor, in order to achieve a reasonable turnoff gain. This is done by implementation of anode shortings or by heavy gold doping of the thick n-base of the GTO. Both measures result in a reduction of the stored charge inside the n-base.

The gate is designed so that charge can be extracted from the p- and n-base via the gate, and that all of the area covered by the cathode can be evacuated very quickly. This and the reduced amount of charge in the base regions is advantageous for a very short turnoff time in ZCS operation. Therefore the switching behavior of the GTO in ZCS should compare favorable to a similarly rated conventional or fast thyristor.

For some of the ZCS modes in Fig. 2, reverse blocking switches have to be used. In an anode shorted GTO, the reverse blocking junction is shorted out. Only gold-doped devices can be used in these applications, unless a diode is connected in series to the GTO.

It was shown in previous papers [1], [7], [9] that for very short hold-off times in ZCS with reverse voltage, it may be necessary to use a switch as shown in Fig. 3 instead of a single GTO, even if the GTO is of the reverse blocking type. If the GTO changes from the on state to the reverse blocking state very quickly, the stored charge is trapped between two blocking junctions and can be removed only by recombination. The central junction is still forward biased in this situation. During the transition from the reverse blocking to the forward blocking state, a forward recovery current will occur to remove the stored charge from the central junction and to make it reverse biased. This forward recovery current can cause the GTO to turn on if the gate drive is not capable to absorb it completely.

The switch in Fig. 3 avoids that the GTO has to block reverse voltage, and the central junction can be brought to a

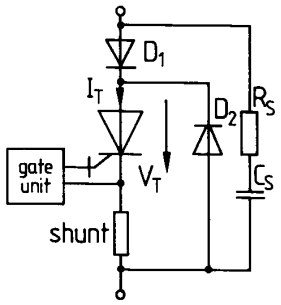

Fig. 3. Improved GTO switch for use in ZCS with reverse blocking voltage.

reverse biased state before the switch has to sustain a forward blocking voltage.

B. Test Circuits

In an experimental investigation, the switching behavior of GTO's in ZCS applications was tested and analyzed. A number of test circuits was used in order to generate the different modes of ZCS in a single shot mode. The circuits are shown in Fig. 4. A GTO 160PFT160 (1600 V, 600 A) was used in all the tests at a current of 300 A peak.

The two circuits at the top of Fig. 4 are used for trapezoidal current waveforms. When T_1 is turned on, the current in L_d and T_1 rises slowly. When the specified value is reached, T_2 is turned on. The current commutates to T_2, and T_1 is turned off in a ZCS mode. The voltage V_c appears as a reverse blocking voltage across T_1 or D_2. Then V_c is rising linearly until it equals V_d. This corresponds to mode 1 in Fig. 2.

If the GTO is used with an antiparallel diode as shown in the second circuit of Fig. 4, the oscillation between L and C continues until D_1 blocks. At this time, V_c has changed polarity and appears suddenly across T_1 as a forward blocking voltage. Thus ZCS mode 2 is obtained.

The component values for modes 1 and 2 are $V_d = 540$ V, $L_d = 1$ mH. L and C were varied from 2.6 μH to 8.9 μH and from 4.7 μF to 10.2 μF, respectively. V_c was also varied between 300 V and 500 V. Thus different waveform parameters such as $dI/dt, dV/dt, tq, V_{\rm rm}$ could be adjusted.

The third circuit in Fig. 4 generates the waveforms of ZCS mode 3. The component values are $V_d = 150$ V, $V_{\rm Cl} = 500$ V, $L_d = 1$ mH, $C = 2.7$ μF and $L = 20$ μH . First T_2 is turned on to build up a current in L_d of approximately 150 A. When T_2 is turned off at $t = t_0, L_d$ acts as a current source, and the voltage across C rises linearly until GTO T_1 is turned on at $t = t_1$. Now a resonant current pulse of the shape

$$I_L = I_{\rm Ld} \cdot (1 - \cos\omega t) + \sqrt{\frac{C}{L}} \cdot V_C(t_1) \cdot \sin\omega t, \quad (1)$$

where $\omega = 1/\sqrt{LC}$, flows through L and T_1. When this current returns to zero, T_1 is turned off. Inbetween the polarity of the voltage across C has reversed and appears as a reverse blocking voltage across T_1 and D_2. Due to the current source L_d, the voltage across C rises linearly until it reaches $V_{\rm Cl}$. With the above component values, an equivalent resonant pulse frequency of about 20 kHz is obtained. The hold-off

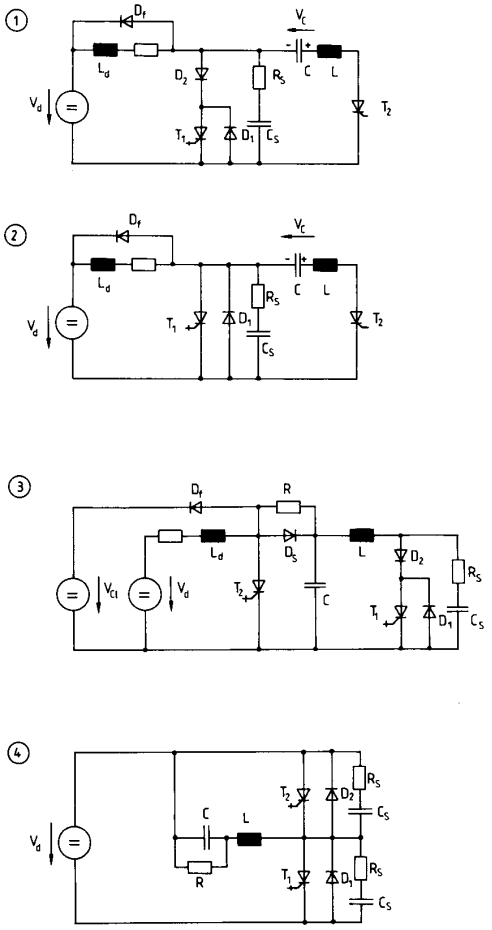

Fig. 4. Test circuits used to generate the switching waveforms in the different ZCS modes.

time can be adjusted by changing the capacitor charging time $(t_1 - t_0)$.

The last circuit in Fig. 4 generates the waveforms of ZCS mode 4. When T_1 is turned on, a sinusoidal current pulse flows through V_d, C, L, and T_1. When the current reverses, T_1 is turned off while D_1 starts conducting. The hold-off interval is terminated when T_2 is turned on and the voltage across T_1 rises very quickly to V_d. In this setup, V_d was 500 V and L and C were chosen to reach a current amplitude of 300 A at various values of the resonant frequency between 10 and 25 kHz.

C. Switching Waveforms

The switching waveforms obtained with GTO's in different modes of ZCS are discussed in the following sections.

Mode 1: Fig. 5 shows the turnoff waveforms of a single GTO in ZCS mode 1, obtained in the first circuit of Fig. 4. After the anode current has fallen from its steady-state value (300 A) to zero, a reverse recovery current makes the gate-cathode junction block very soon, and the anode voltage steps to the gate-cathode breakdown voltage. When the anode-side junction is also free of excess carriers, the anode voltage jumps

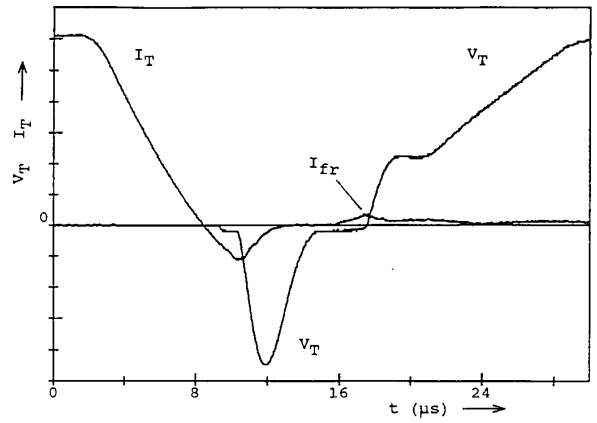

Fig. 5. Turnoff waveforms of reverse blocking GTO in ZCS mode 1. I_T = 50 A/Div, V_T = 100 V/Div.

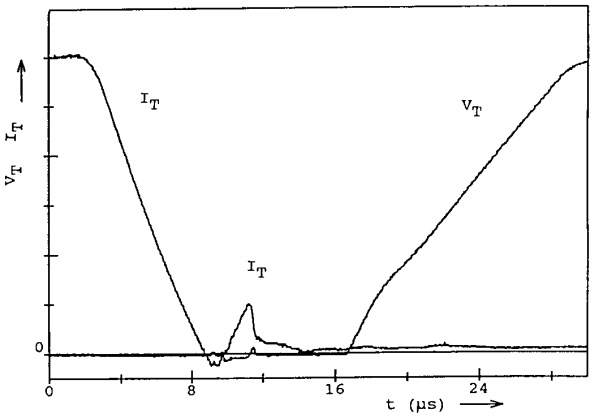

Fig. 7. Turnoff waveforms of a GTO in a switch according to Fig. 3 (ZCS mode 1). I_T = 50 A/Div, V_T = 100 V/Div.

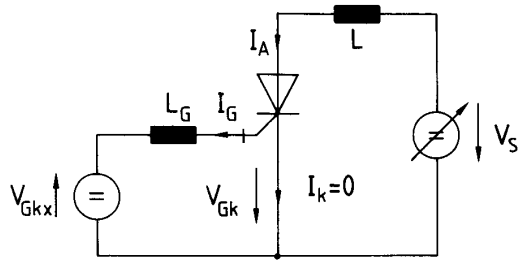

Fig. 6. Equivalent circuit of the GTO and its environment during the forward recovery in ZCS modes 1 and 3.

to the commutation capacitor voltage. The step is smoothed by the RC snubber. The forward recovery process begins when the anode voltage has risen to almost zero. Now the anode current increases while the anode voltage remains constant until the central junction blocks. Then a step in anode voltage occurs, and afterwards the anode voltage rises linearly with the commutation capacitor voltage. During this time, a tail current is observed.

Fig. 6 is used to discuss the operation conditions necessary for keeping the device in the off state during forward recovery. V_s is rising linearly at a rate dV_s/dt. A current starts to flow when V_s equals $-V_{\mathrm{GK}x}$. The anode current equals the gate current as long as $V_{\mathrm{GK}} < 0$. If the gate-cathode voltage becomes positive, a cathode current may flow and may turn on the device.

The analysis of this circuit reveals that the device can be held in the off state when

$$\frac{dV_s}{dt} \leq \sqrt{\frac{V_{\mathrm{GK}x}^3 \cdot (L + L_G)^2}{6 \cdot Q_f \cdot L_G^3}} \tag{2}$$

where Q_f is the forward recovery charge that has to be removed from the central junction in order to attain blocking capability. Q_f depends on many parameters like the on-state current, the reverse recovery current, the hold-off time and the recombination time constant. For a certain operation condition, Q_f can be measured via the forward recovery current amplitude I_{fr} using the equation

$$Q_f = \frac{1}{6}\sqrt{\frac{8 \cdot I_{\mathrm{fr}}^3 \cdot (L + L_G)}{dV_s/dt}}. \tag{3}$$

In this mode of operation, losses occur during reverse recovery, forward recovery and tail time.

Fig. 7 shows the turnoff waveforms in the same circuit, but using a switch as shown in Fig. 3. Now the reverse voltage is blocked by the series diode, and the reverse recovery current of this diode is flowing through the antiparallel diode. During the hold-off time, the voltage across the GTO is zero. When the negative gate voltage is applied, the gate-cathode junction blocks almost instantaneously because the cathode current is zero. The negative gate voltage drives a current through the antiparallel diode, into the anode and out of the gate of the GTO. This current removes charge from the central junction and makes it reverse biased while anode voltage is zero. Turnoff losses occur only when the anode voltage is rising and are widely reduced as compared to conventional GTO operation because the tail current is reduced significantly [1], [7], [9].

Mode 2: In Fig. 8, the switching waveforms obtained in the second circuit of Fig. 4 are shown. They look quite similar to those in Fig. 7, with the difference that the anode voltage rises very quickly after the hold-off time. As a result, the tail current is larger in the first few microseconds of the voltage risetime.

The next two figures show sinusoidal current waveforms of 300 A peak. In this case the excess carrier density inside the device cannot reach its steady state value as in the case of trapezoidal current because the peak current is flowing only for a few microseconds. In addition, the stored charge has more time to recombine during the current fall.

Mode 3: In the third circuit of Fig. 4, a reverse blocking GTO could be used without series and antiparallel diodes because the large series inductance and the reduced stored charge make it easy to keep the device in the off-state during the forward recovery. However, the forward recovery time t_{fr}

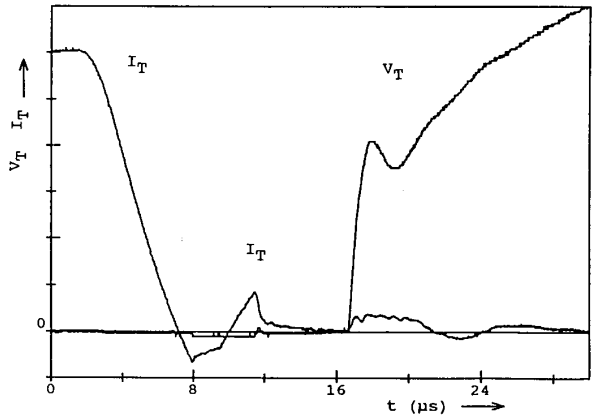

Fig. 8. Turnoff waveforms of a GTO in ZCS mode 2. I_T = 50 A/Div, V_T = 100 V/Div.

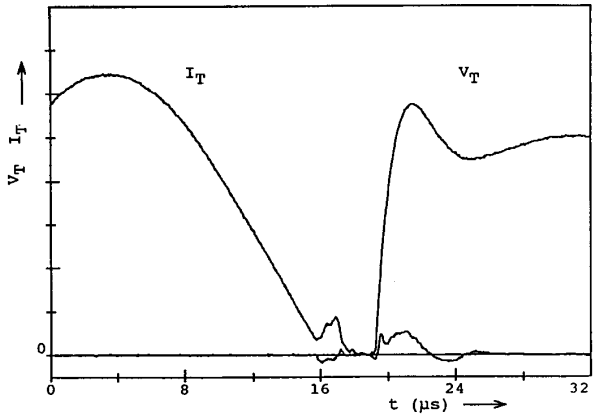

Fig. 10. Turnoff waveforms of a GTO in ZCS mode 4. I_T = 50 A/Div, V_T = 100 V/Div.

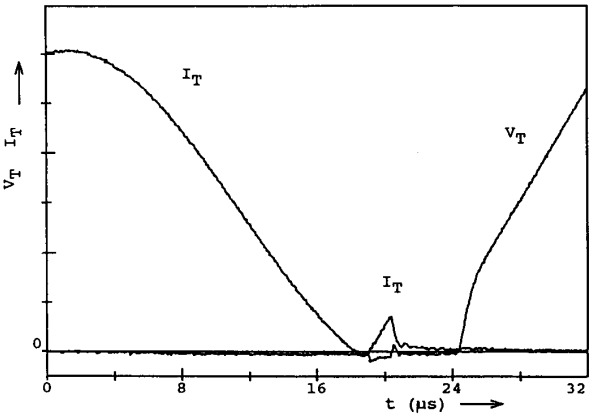

Fig. 9. Turnoff waveforms of a GTO in a switch according to Fig. 3 in ZCS mode 3. I_T = 50 A/Div, V_T = 100 V/Div.

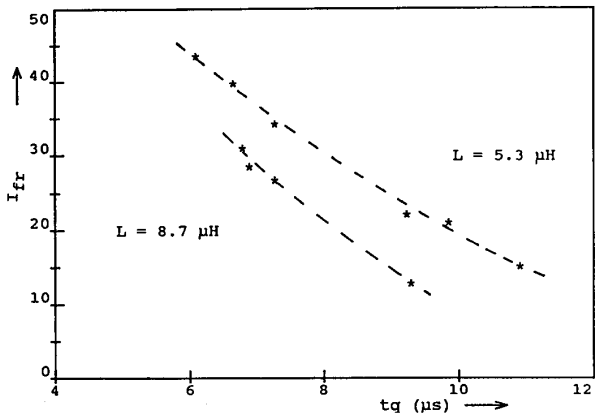

Fig. 11. Forward recovery current of the GTO in mode 1 as a function of $t_q \cdot I_{\mathrm{Tpk}}$ = 300 A, C = 6.9 µF, V_c variable.

depends only slightly on L and Q_f:

$$t_{\mathrm{fr}} = \sqrt[3]{\frac{6 \cdot Q_f \cdot (L + L_G)}{dV_s/dt}}. \tag{4}$$

The time t_{fr} is adding to a minimum off time of the device that has to pass before the device can be turned on again. Especially in the RDCCLI, this is a major drawback because it increases all the component ratings of the circuit. Therefore it is advisible to use the switch configuration in Fig. 3.

Fig. 9 shows the turnoff waveforms obtained in the third circuit of Fig. 4 when the improved switch is used. The reduced amount of stored charge is reflected in the reduced peak current during the hold-off time. Surprisingly there is almost no tail current when the anode voltage rises. Therefore the switching losses are very small in this application. The operating conditions in the RDCCLI seem to be very favorable for a GTO.

Mode 4: In Fig. 10, the waveforms obtained in the last test circuit of Fig. 4 are shown. It seems that the amount of stored charge is larger as compared to Fig. 9 (mode 3), which may result from the steeper dI/dt. Since the voltage rises very quickly after the hold-off time, the tail current is much larger than in Fig. 9 as was expected. However, a comparison to the ZCS modes 1 and 2 (trapezoidal current) shows that the duration of the tail current is much shorter and the losses can be expected to be much lower.

D. Investigation of Device Characteristics

Using the test circuits shown in Fig. 4, some device characteristics were analyzed systematically. The investigation focussed on the behavior of a single GTO in ZCS mode 1, on the charge that has to be extracted via the gate during turnoff, and, most important, on the switching losses in the different ZCS modes.

The forward recovery current amplitude I_{fr} of a reverse blocking GTO used in ZCS mode 1 is depicted in Fig. 11 as a function of the hold-off interval t_q. As expected, I_{fr} falls when t_q increases (a result of the recombination of excess carriers during t_q). It is also visible that a large series inductance L is important for keeping I_{fr} within limits, as indicated by (3). Fig. 11 also shows that the device can be used at t_q down to 6 µs without danger of accidental turn-on.

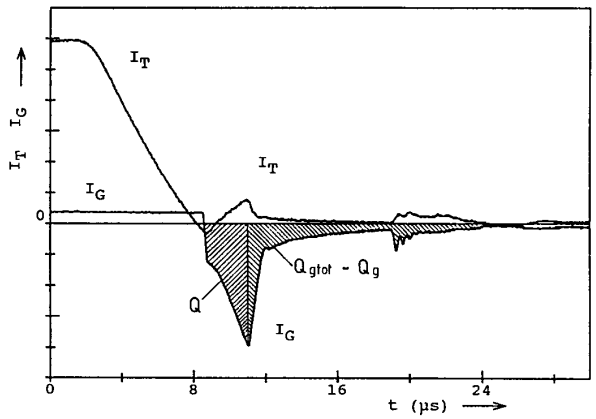

Fig. 12. Anode current and gate current of the GTO in mode 2. I_T: 50 A/div, I_G : 10 A/Div.

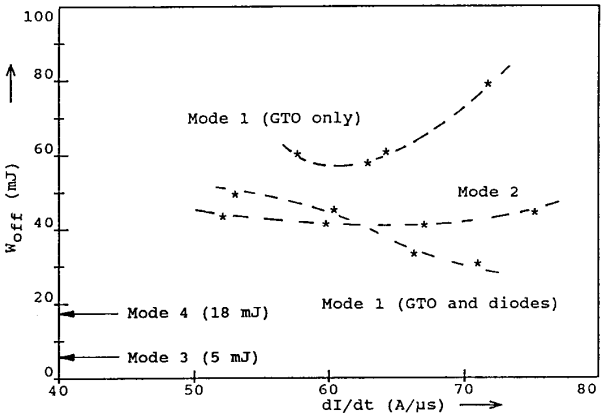

Fig. 14. Switching losses of the GTO in ZCS modes 1 and 2 as a function of dI/dt. $I_{\mathrm{Tpk}} = 300$ A, $L = 5.3$ μH, $C = 6.9$ μF, V_c variable.

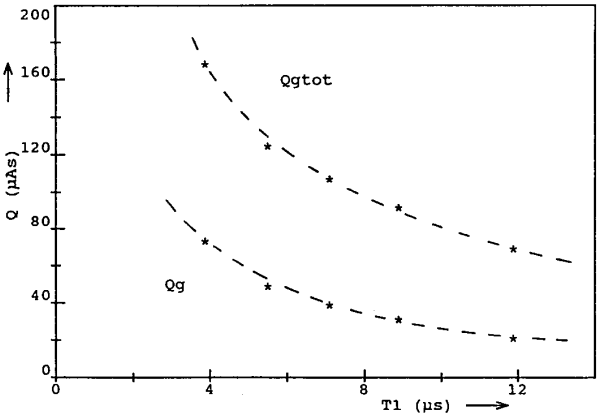

Fig. 13. Gate charge in mode 2 as a function of the time when the negative gate current is applied. $I_{\mathrm{Tpk}} = 300$ A, $L = 5.3$ μH, $C = 10.2$ μF, $V_C = 450$ V.

The amount of charge that flows out of the gate into the gate drive is important for the power rating of the gate unit. This charge depends on the time when the negative gate signal is applied. The gate current was measured in ZCS mode 2 for different time intervals T_1 between the start of the current fall ($I_T = 90\%\ I_{\mathrm{Tpk}}$) and the beginning of the negative gate current.

Fig. 12 presents the anode and gate currents at $T_1 = 5.5$ μs. Note that anode current and gate current are almost equal during the hold-off time. When the anode voltage rises at about $t = 20$ μs, a displacement current is seen in both current waveforms. The gate charge for different values of T_1 is plotted in Fig. 13. Both Q_g (the charge extracted from the gate before the maximum gate current is reached) and $Q_{g\mathrm{tot}}$ (the total amount of charge flowing out of the gate of the GTO) decrease exponentially.

The power needed for the reverse gate drive can be estimated to

$$P_g = f \cdot Q_{g\mathrm{tot}} \cdot V_{GKx} \leq 3\ \mathrm{W/KHz} \qquad (5)$$

at $I_{\mathrm{Tpk}} = 300$ A. This small amount of gate drive power is an important benefit of ZCS with GTO's. For instance at 10 kHz, only 30 W of reverse gate drive power would be necessary.

Switching Losses: The switching losses have been investigated in all the different ZCS modes. For a given set of L and C, the turnoff losses in mode 1 and 2 are shown in Fig. 14 as a function of dI/dt of the anode current. For comparison, the turnoff loss under conventional gate turnoff at 300 A using a 1 μF snubber capacitor is about 80 mJ (data sheet information).

It is not surprising that a reverse blocking GTO used in mode 1 shows the largest amount of switching losses, because a large portion of the losses is generated during the reverse recovery. This portion increases with dI/dt because a larger dI/dt is obtained from a higher commutation voltage V_c (see Fig. 4). When the GTO is used in a switch as shown in Fig. 3, losses occur only during forward recovery. Here the losses are lower at large values of dI/dt because the hold-off time increases almost proportionally with V_c and dI/dt. The losses in mode 2 are found to be almost constant. This is because there is a larger step in the forward blocking voltage when the commutation voltage is larger. Thus two effects (larger t_q, larger voltage step) compensate each other.

In ZCS mode 4, the turnoff losses were investigated as a function of the equivalent pulse frequency, the hold-off interval, and the start of the negative gate current. Surprisingly the losses were almost constant during all the experiments. Although the equivalent pulse frequency was varied between 8 and 22 kHz, the hold-off time between 2 and 10 μs and the start of the negative gate current through the complete range of the hold-off time, a significant dependance of the losses on one of these parameters could not be found. The turnoff losses were 18 mJ at 10 kHz and 21 mJ at 20 kHz. This is only half of the losses obtained in ZCS mode 1 and mode 2.

The most remarkable result, however, is the switching loss in ZCS mode 3 when the GTO is used in the configuration of Fig. 3. At a current amplitude of 300 A, an equivalent pulse frequency of 20 kHz, and hold-off times of approximately 6 μs, the turnoff losses are as low as 5 mJ. This is only one quarter of the losses in mode 4 and about one eighth of the losses in modes 1 and 2! The explanation for these very good results is found in the short duration of the peak current, the

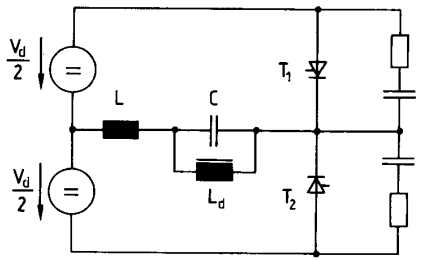

Fig. 15. Test circuit for ZCS mode 3 in continuous operation.

smooth decrease of anode current, and the soft rise of anode voltage.

In conclusion, it can be stated that ZCS mode 3, which is obtained in the resonant dc current link inverter, is the most convenient mode of ZCS for a GTO.

IV. Behavior of SCR's in a New ZCS Mode

We have seen in the previous section that the operation mode 3 of Fig. 2 is very convenient for a GTO. It is very likely that also an SCR may benefit from this ZCS mode. Therefore the behavior of SCR's in the RDCCLI was also investigated.

A test circuit according to Fig. 15 was set up in order to generate the waveforms typical for a RDCCLI in continuous operation. In this circuit, the current source is realized by a large inductance L_d (45 mH). When T_1 and T_2 are off, the current source L_d charges the capacitor C linearly. A resonant current cycle is started by turning on either T_1 or T_2. The sinusoidal current pulse is flowing via L, C, $V_d/2$ and T_1 or T_2. The current in L_d increases when T_1 is switched and decreases when T_2 is switched. This provides efficient control on the current I_{Ld}. V_d was chosen at 230 V, L at 61 μH and C at 500 nF and 900 nF, such that two different pulse frequencies were realized.

When only I_{Ld} is changed and the time intervals between two pulses are kept constant, the amplitudes of the current and voltage waveforms change proportionally to I_{Ld}, while the timing and shape of the pulses is constant. Of course also dI/dt and dV/dt are changed proportionally.

A symmetrical fast turnoff thyristor IR 81RM100 rated at 125 A RMS and 1000 V was used in the experiment. Peak currents between 30 A and 115 A were obtained at pulse frequencies of 20 and 27 kHz. For the lower frequency, a constant reverse recovery time of only 1.5 μs at a peak reverse recovery current of less than 2 A was measured over the complete peak anode current range. The hold-off time during which the device is kept in the reverse blocking state could be reduced to only 6 μs, while the data sheet specification of t_q was 20 μs. However, at increased temperature and high peak currents the devices failed to turn off, a result of the temperature dependent carrier concentrations. For safe operation at rated current, the hold-off time would have to be increased.

At the higher frequency, the reverse recovery time t_{rr} was constant at 2 μs approximately, while the peak reverse recovery current I_{rr} changed as indicated in Fig. 16. The figure also shows how dI/dt is rising proportionally with the current amplitude I_{Tpk}. The hold-off time was again 6 μs for all currents. The rate of rise of the reapplied forward voltage was 50 V/μs worst case. These results were obtained without any negative voltage across the gate during turnoff.

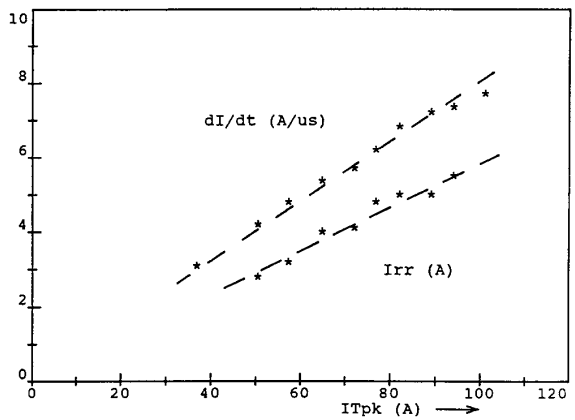

Fig. 16. Reverse recovery current I_{rr} of SCR 81RM100 and dI/dt of the anode current waveform as a function of the peak anode current I_{Tpk}.

In all cases the turn-on losses were seen to be very small, below 1 mJ, and the turnoff losses were even smaller and could hardly be measured.

The reason for the good behavior of the SCR in this new application is the large inductance in series with the device, and the slow decrease of current prior to turnoff. The latter allows the stored charge almost to follow the instantaneous current level, and thus only few charge is stored in the base regions when turnoff occurs. This and the large inductance help to keep the forward recovery current small, so that the device is not turned on again although the forward recovery current is flowing completely via the gate-cathode junction.

V. Conclusion

The application of GTO's in different modes of ZCS was investigated. It is possible to achieve hold-off times much smaller than for thyristors if the GTO is used in combination with an antiparallel diode. In ZCS modes with trapezoidal current, the switching losses can be widely reduced if the hold-off time is several microseconds long. In that case, an increase in switching frequency over the limits for GTO's and for thyristors is possible. The operation conditions are much more convenient in the case of sinusoidal current. The application where the device stresses during the switching transitions are smallest is the Resonant dc Current Link Inverter. Here turn-on and turnoff losses are very small, even for very short hold-off times, and the switching frequencies can be pushed far above the limitations known so far. The drawback is ,that a series diode has to be used in order to have a reverse blocking switch. This increases both the number of devices and the conduction losses of the switch.

An additional investigation was carried out on the behavior of SCR's in the RDCCLI. In this application, the device can be used with hold-off intervals much shorter than specified as t_q. However, a GTO still has the advantage of shorter hold-off

times that can even be reduced down to zero. The selection of a device for a zero current switching application is thus a trade-off between high frequency and low conduction loss and complexity.

ACKNOWLEDGMENT

The authors would like to thank F. Ransmann for carrying out most of the experimental work.

REFERENCES

[1] S. M. Tenconi, M. Zambelli, L. Malesani, and P. Tenti, "The reverse blocking GTO as a very fast turn-off thyristor," in *Proc. IEEE-IAS Ann. Meeting*, 1986, pp. 377–383.
[2] L. Malesani and P. Tenti, "Medium frequency GTO inverter for induction heating applications," in *Proc. EPE*, 1987, pp. 271–276.
[3] Thomson Semiconductors, "ZTO: A new high power component," "ZTO: New perspectives for high power conversion," "Optimal use of a ZTO," Application Notes, 1987.
[4] Marconi Electronic Devices, "The ZTO zero turn-off thyristor," Application Notes, 1987.
[5] C. Millour and J. P. Abgrall, "New perspectives for power converters with ZTO thyristors," Application Notes, 1988.
[6] K. E. Bornhardt, "Switching behavior of a pulse-commutated GTO," in *Proc. Inst. Elect. Eng.-PEVD*, London, U.K., 1988, pp. 83–86.
[7] J. P. Pascal, G. Coquery, and R. Lallemand, "Increasing frequency using GTO in gate-assisted turn-off mode," in *Proc. Inst. Elect. Eng.-PEVD*, London, U.K., 1988, pp. 87–90.
[8] Y. Murai and T. Lipo, "High frequency series resonant dc link power conversion," *Proc. IEEE-IAS Ann. Meeting*, 1988, pp. 648–656.
[9] A. Mertens and H.-C. Skudelny, "Switching losses in a GTO inverter for induction heating," in *Proc. IEEE PESC'89*, Milwaukee, WI, pp. 91–98.
[10] ——, "Operation and control requirements for a GTO used in a parallel resonant inverter for induction heating," in *Proc. EPE*, Aachen, Germany, 1989, pp. 1097–1102.
[11] L. Malesani and R. J. Morris, "Design and characterization of GTO devices for medium frequency applications," in *Proc. EPE*, Aachen, Germany, 1989, pp. 115–120.
[12] R. J. Morris and F. J. Wakeman, "A new family of GTO devices for medium frequency applications," in *Proc IEEE-IAS Ann. Meeting*, San Diego, CA, 1989, pp. 1264–1269.

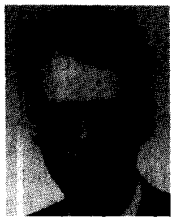

Axel Mertens (S'89–M'93) received the Dipl.-Ing. degree in 1987 and the Dr.-Ing. degree in 1992 with honors from the RWTH Aachen University of Technology, Germany.

From 1988 to 1992 he was a Research Engineer at the Institute for Power Electronics and Electric Drives at the RWTH, Aachen, where he worked on resonant power converters, devices, and modulation strategies. In 1989, he was a Research Associate at the University of Wisconsin–Madison and a fellow of the German VDE–ETG. In 1993 he joined Siemens AG in Erlangen, Germany, where he is currently working as an R&D Engineer in the field of control electronics for ac drives.

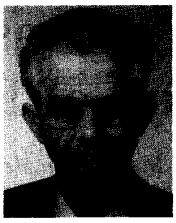

Hans-Christoph Skudelny(M'79–SM'91) received the Dipl.-Ing. degree in 1957 and the Dr.-Ing. degree in 1960 from the RTWH Aachen University of Technology, Aachen, Germany.

From 1961 to 1973 he was with Brown Boveri & Cie. AG, Mannheim, Germany, where he worked in the fields of power electronics and traction. He became a Professor and head of the Institute for Power Electronics and Electric Drives at Aachen University of Technology in 1973. His main research interests are converter circuits, industrial and traction drives, and battery-powered electric vehicles.

Paulo P. A. Caldeira (S'86–M'90) received the B.E.E. degree in 1979 from the Universidade Federal of Rio Grande do Sul, Brazil, and the M.S.E.E. degree in 1985 from the Universidade Federal of Rio de Janeiro, Brazil. He received the Ph.D. degree in electrical engineering from the University of Wisconsin-Madison, in 1990.

From 1980 to 1986 he was employed by Petrobras S.A. as an Equipment Engineer and was involved in maintenance, specification, and design of drive systems for the oil-drilling industry. He also worked as a Project Engineer in the area of drive systems for the paper industry at Marquip, Inc., Madison, WI. He is currently a Senior Member of the Research Staff at Philips Laboratories, Briarcliff Manor, NY. His research interests are in switching and resonant converters, electric machine drives, microelectronics, and electromagnetic interference.

Dr. Caldeira is a member of the Tau Beta Pi Engineering Honor Society and the IEEE Power Electronics Society.

T. Lipo (M'64–SM'71–F'87), photograph and biography not available at the time of publication.